

**IMECE2004-60735**

## **DECENTRALIZED VIBRATION CONTROL WITH NETWORKED EMBEDDED SYSTEMS**

Tao Tao, Isaac Amundson, Kenneth D. Frampton  
Vanderbilt University, Nashville, TN 37235

### **ABSTRACT**

The early promise of centralized active control technologies to improve the performance of large scale, complex systems has not been realized largely due to the inability of centralized control systems to “scale up”; that is, the inability to continue to perform well when the number of sensors and actuators becomes large. Now, recent advances in Micro-electro-mechanical systems (MEMS), microprocessor developments and the breakthroughs in embedded systems technologies, decentralized control systems may see these promises through. A networked embedded system consists of many nodes that possess limited computational capability, sensors, actuators and the ability to communicate with each other over a network. The aim of this decentralized control system is to control the vibration of a structure by using such an embedded system backbone. The key attributes of such control architectures are that they be scalable and that they be effective within the constraints of embedded systems. Toward this end, the decentralized vibration control of a simply supported beam has been implemented experimentally. The experiments demonstrate that the reduction of the system vibration is realized with the decentralized control strategy while meeting the embedded system constraints, such as a minimum of inter-node sensor data communication, robustness to delays in sensor data and scalability.

### **INTRODUCTION**

The vibration of structures is a very important problem in mechanical engineering, structural engineering, and especially aerospace engineering. There has been a great deal of interest in vibration control of structures in the past decades, and most methods can be categorized into the following two strategies: the attenuation of the noise source, and the attenuation of the noise at the reception location. Passive vibration control, which uses passive elements to change the system damping and stiffness, has been widely used. Although no power source is needed in passive vibration control, the weight of the whole

system is often increased which is not acceptable in aerospace applications.

Due to the limitations of passive vibration control, active vibration control was introduced. Most active control designs rest on the presupposition of centrality: one digital computer is used to process the data from all sensors and generate the control forces in order to implement the control algorithm. Centralized control technology is applicable to small and medium sized systems. However, when a large-scale system is considered, it is very difficult for one computer to meet the overwhelming need for processing efforts. Therefore, there is a trend toward decentralized control for increased reliability and better processing performance. A decentralized control system consists of many embedded microprocessors, sensors and actuators. Depending on the information from the local sensor, a microprocessor will implement some control strategy and generate a control force through an actuator. There has been extensive research on the application of active materials to the vibration control of flexible structures. Swigert and Forward used lead zirconate titanate (PZT) as the active damper to control the mechanical vibration of an end-supported mast [1]. Bailey and Hubbard developed the active vibration control system for a cantilever beam using Poly Vinylidene Fluoride (PVDF) [2]. Amant and Cheng used a FIR controller based on LMS to control the vibration of a plate [3]. Choi performed vibration control with multi-step Bang-Bang control [4].

For embedded control systems, the microprocessors used are usually restricted by the available space and power supply, and the control forces are calculated only from the local sensor information. The technological advances of embedded systems and reduced cost of MEMS devices make it possible to realize decentralized control systems in which the local control force is calculated according to the information not only from its local sensor but also from neighboring sensors as well. A model of such decentralized control systems is illustrated in Fig. 1.

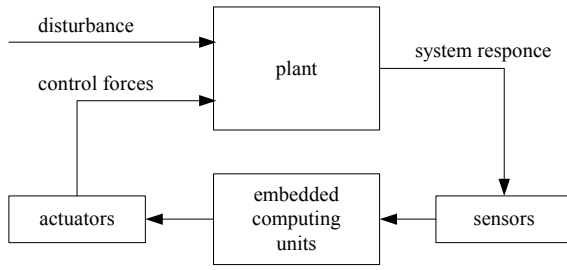


Figure 1: Concept of decentralized control

Decentralized control systems consist of many nodes, each including a computing unit, a sensor and an actuator. All nodes can communicate with each other, so that a node can send its local sensor data to other nodes and receive sensor data from other nodes [5]. When the control system is running, every node in the system will first communicate with each other and calculate its own location, so that a networked embedded system is established. Some disturbance will then cause the plant to vibrate, and the sensors will measure the system response. Each node will send its local sensor data to some specific group of nodes, which is predetermined by the chosen communication configuration. Then the computing unit in each node will implement some control algorithm, such as LQR control, according to its local sensor data and sensor data received from other nodes. The actuators will apply control forces on the plant to complete the feedback control structure.

## MODELING OF PHYSICAL SYSTEM

In order to reduce the vibration of structures using decentralized control, it is necessary to have knowledge of the system dynamics. For active vibration control, the physical system includes not only the structure, such as beam and plate structures, but also sensor and actuator devices. Therefore the dynamics of sensor and actuator devices should be considered in order to achieve successful controller design.

### Piezoelectric Actuators

Many different active transduction materials have been used in various fields, such as shape memory alloy (SMA). However, the most commonly used transduction material is piezoelectric material, and it has been used widely for active vibration control systems.

Piezoelectric materials have some important characteristics: direct piezoelectric effect and inverse piezoelectric effect. When the piezoelectric material has an external load applied, it becomes electrically polarized. Thus, an electrical charge is produced at the surface of the material. This phenomenon is called direct piezoelectric effect, which is utilized for the design of piezoelectric sensors. Conversely, when a voltage is applied to a piezoelectric material, it will induce a strain in the material. This phenomenon is called inverse piezoelectric effect, which is utilized for the design of piezoelectric actuators. Since the direct and inverse piezoelectric effects are designed to be linear over the range of the application, it is very

convenient to measure the change of electric field or mechanical load.

Some example piezoelectric materials are natural quartz crystals, polycrystalline piezoceramic and semicrystalline polyvinylidene polymer. The most commonly used piezoelectric materials are usually made from two materials: PZT and PVDF. Different piezoelectric materials have different characteristics, so it is very important to choose an appropriate material. Since a simply supported aluminum beam is the structure considered in this experiment, small patches of PZT are attached to the beam surface and used as the actuators. In order to get maximum control forces from the PZT actuators, the actuator patches are driven in couples by the voltage, which is demonstrated in Fig. 2 [6].



Figure 2: PZT actuators driven in couples

Pairs of PZT actuators are attached to both sides of the beam at the same horizontal locations. When a drive voltage is connected to the PZT pairs in the way shown in Fig. 2, these two actuators have opposite deformation. For example, the extension of the upper actuator and the contraction of the lower actuator will cause the beam structure to bend more than with only one actuator in place.

### Modeling of a Simply Supported Beam

The vibrating structure under consideration is a simply supported beam, which is modeled using Galerkin's technique:

$$0 = EI\nabla^4 w(x,t) + \rho h \frac{\partial^2 w(x,t)}{\partial t^2} + f_d(x,t) + \sum_{k=1}^K f_c(x,t) \quad (1)$$

where  $w(x,t)$ ,  $E$ ,  $I$ ,  $\rho$  and  $h$  are the beam displacement, modulus of elasticity, moment of inertia, density and thickness, respectively. The beam is acted upon by a disturbance force,  $f_d$ , and control forces,  $f_c$ .

The mode shape of the simply supported beam is described as:

$$\Psi_n(x) = \sin\left(\frac{n\pi}{l}x\right) \quad (2)$$

A separable solution is assumed using the *in vacuo* beam eigenfunctions and generalized coordinates of the form

$$w(x,t) = \sum_{n=1}^N \Psi_n(x) q_n(t) = \sum_{n=1}^N \sin\left(\frac{n\pi x}{L}\right) q_n(t) \quad (3)$$

where  $q_n(t)$  are the generalized coordinates. Substituting Eq. (3) into Eq. (1), multiplying by an arbitrary expansion function,  $\Psi_r(x,y)$ , and integrating over the domain yields a set of ordinary differential equations of the form [7]:

$$0 = M_s \ddot{q}_n(t) + K_s q_n(t) + \sum_{k=1}^N Q_{kn}^c(t) + Q_n^d(t) \quad (4)$$

where  $M_s$  and  $K_s$  are the modal mass and stiffness and  $Q_{kn}^c$  and  $Q_n^d$  are the control generalized forces and the disturbance generalized forces.

The mass matrix for the beam system is derived as follows:

$$\begin{aligned} M_s(p, q) &= \int_0^l \int_0^w \int_0^h \Psi_r^T(x) \rho_s(x) \Psi_r(x) dx dy dz \\ &= \rho w h \int_0^l \sin\left(\frac{p\pi}{l}x\right) \sin\left(\frac{q\pi}{l}x\right) dx \\ &= \begin{cases} \frac{\rho l w h}{2} & \text{when } p = q \\ 0 & \text{when } p \neq q \end{cases} \end{aligned} \quad (5)$$

The stiffness matrix for the beam system is expressed as:

$$K_s(p, q) = \begin{cases} \frac{p E h^3 w \pi^4}{24 l^3} & \text{when } p = q \\ 0 & \text{when } p \neq q \end{cases} \quad (6)$$

Equation (4) can be cast into state space form [8]:

$$\begin{cases} \dot{x} = Ax + Bu \\ y = Cx + Du \end{cases} \quad (7)$$

The state vector is described as:

$$x = [r \quad \dot{r}]^T \quad (8)$$

where  $r$  is the vector of generalized mechanical coordinates.

The input vector consists of disturbance and control forces at all actuators:

$$u = [F_{disturbance} \quad F_1 \quad F_2 \quad \dots \quad F_{50}]^T \quad (9)$$

The matrix A can be expressed as:

$$A = \begin{bmatrix} 0 & I \\ -[M_s]^{-1} K_s & -2\xi \sqrt{[M_s]^{-1} K_s} \end{bmatrix} \quad (10)$$

where proportional damping has been added to each mode in the above equation.

The matrix B for the simulated beam is expressed as:

$$B = \begin{bmatrix} 0 & 0 \\ I & [M_s]^{-1} \Theta \end{bmatrix} \quad (11)$$

where the coupling matrix is defined as:

$$\Theta = \begin{bmatrix} \sin(1 \times l_1 \times \pi) & \sin(1 \times l_2 \times \pi) & \dots & \sin(1 \times l_k \times \pi) \\ \sin(2 \times l_1 \times \pi) & \sin(2 \times l_2 \times \pi) & \dots & \sin(2 \times l_k \times \pi) \\ \vdots & \vdots & \vdots & \vdots \end{bmatrix} \quad (12)$$

and  $l_k$  are the coordinates of actuators along the beam.

The matrices C and D depend on the choice of observed outputs, and can be modified to observe any set of variables desired. The matrix D is usually a zero matrix.

Since digital microprocessors are used in the decentralized control systems, the continuous state space equations need to be transformed to discrete-time state space equations:

$$\begin{cases} x_{k+1} = Gx_k + Hu_k \\ y_k = Cx_k + Du_k \end{cases} \quad (13)$$

## DECENTRALIZED CONTROL SYSTEM DESIGN

There are a lot of different strategies to design a stable control system [9], and the design of the control systems in this simulation is based on quadratic performance indexes. For an active vibration control system, the system dynamics can be expressed in state space equations:

$$\dot{x}(t) = Ax(t) + Bu(t) \quad (14)$$

$$y(t) = Cx(t) \quad (15)$$

where  $x$  is the state vector,  $u$  is the control vector,  $y$  is the output vector, and A, B, C are system matrices.

The objective of control system design is to minimize the performance index by choosing the control vector  $u(t)$ . The standard infinite time quadratic performance index is defined as follows [10]:

$$J = \frac{1}{2} \int_0^{\infty} [x'(t) Q x(t) + u'(t) R u(t)] dt \quad (16)$$

where J is the performance index, Q is a positive-definite (or positive-semidefinite) Hermitian or real symmetric matrix, and R is a positive-definite Hermitian or real symmetric matrix.

The control vector  $u(t)$  usually depends on the output vector  $y(t)$ , and the relationship between the output vector and control vector can be expressed as:

$$u(t) = -Ky(t) \quad (17)$$

where  $K$  is the feedback gain matrix.

From previous equations, it is shown that the performance index  $J$  is related to the feedback gain matrix. In order to optimize the performance of control systems, the optimal feedback gain matrix should be chosen to minimize the performance index. The algorithm for computing the optimal feedback gain matrix was first presented in the article by Levine [11].

From Eq. (14), (15) and (17), the state space equation for the system can be rewritten as:

$$\dot{x}(t) = [A - BKC]x(t) \quad (18)$$

The state vector  $x(t)$  can be expressed as:

$$x(t) = \Phi(t)x(0) \quad (19)$$

where  $\Phi(t)$  is the fundamental transition matrix for the system, and it is defined as:

$$\Phi(t) = e^{[A-BKC]t} \quad (20)$$

Substituting Eq. (18) and (19) into Eq. (16), the performance index can be rewritten as:

$$J = x'(0) \left[ \frac{1}{2} \int_0^\infty \Phi'(t) (Q + C' K' R K C) \Phi(t) dt \right] x(0) \quad (21)$$

It is shown in Eq. (21) that the performance index depends both on the feedback gain matrix  $K$  and the initial state  $x(0)$ . The initial state  $x(0)$  cannot be controlled, and it can be assumed to be a random variable which uniformly distributes on the surface of the dimensional unit sphere. By averaging performance indexes with independent initial states, the initial state  $x(0)$  can be eliminated from Eq. (21). Accordingly, in order to optimize the performance and minimize the performance index, we just need to consider the feedback gain matrix  $K$ .

From Eq. (21), the following equation can be derived [11]:

$$K_{n-1} = R^{-1} B' F_{n-1} L_{n-1} C' [C L_{n-1} C']^{-1} \quad (22)$$

where  $F_{n-1}$  is the solution of

$$F_{n-1} [A - BK_{n-2} C] + [A - BK_{n-2} C] F_{n-1} + Q + C' K_{n-2}' R K_{n-2} C = 0 \quad (23)$$

and  $L_{n-1}$  is the solution of

$$L_{n-1} [A - BK_{n-2} C] + [A - BK_{n-2} C] L_{n-1} + I = 0 \quad (24)$$

With Eq. (22), (23) and (24), we can obtain the optimal feedback gain matrix  $K$ , which makes the control system stable. In order to get the optimal feedback gain for a known system, the first step is guessing an initial value  $K_0$  for  $K$ , then according to Eq. (23) and (24),  $F_1$  and  $L_1$  can be calculated. Substituting  $F_1$  and  $L_1$  into Eq. (22), we can get  $K_1$ . If the control performance with feedback gain  $K_1$  is good enough, then  $K_1$  is the expected optimal feedback gain matrix. Otherwise,  $K_1$  is used as the initial value to obtain  $K_2$ ,  $K_3 \dots$  until the expected control performance is achieved.

The strategy described above has been demonstrated satisfactorily and is used in this simulation to get the optimal feedback gain.

## EXPERIMENTAL IMPLEMENTATIONS

The verification of distributed vibration control was performed with a simply supported beam shown in Fig. 3. The experimental setup consists of six major functioning units: a beam, sensors, anti-aliasing circuits, microprocessors, amplifiers and actuators.

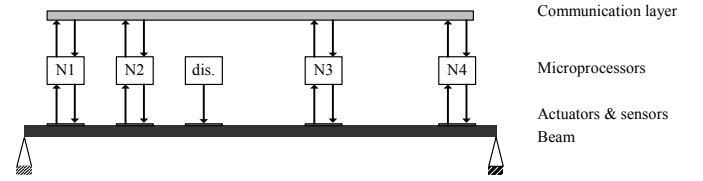


Figure 3: Decentralized vibration control of a simply supported beam

The physical properties of the flexible aluminum beam are given in Table 1. The beam was machined with knife-edges near the ends to provide the pinned supports.

Table 1: Physical properties of the beam

Parameters	Value
Young's Modulus $E$	73.1 GPa
Density $\rho$	2770 kg/m <sup>3</sup>
Length $L$	1 m
Width $b$	5.08e-2 m
Thickness $h$	3.175e-3m

The vibration of the beam was measured by four accelerometers attached to the beam surface. In order to optimize the control performance, the placement of the sensors should be considered. Sensors were not evenly distributed along the beam. The actual locations of the sensors were 0.125m, 0.25m, 0.688m and 0.875m (the distance from the left end of the beam to the centers of the sensors).

The data acquired at each sensor was filtered and amplified through a circuit board before being transmitted to the corresponding microprocessor. Since the vibrating structure is

controlled in the frequency range of between 0-250Hz in these experiments, the cutoff frequency of the 2<sup>nd</sup> order Chebyshev anti-aliasing filter is set to 250Hz in order to minimize the aliasing effect. Although there is an internal amplifier in the accelerometer, the voltage readout representing the structure vibration at each sensor was still small (in the milli-volt range). The filtered data was amplified appropriately, so that the measuring range of the A/D circuit in the microprocessor could be utilized and the measuring resolution improved correspondingly.

The Prometheus boards from Diamond Systems Corporation were used as the microprocessor nodes for this research. Each board is a high-integration PC/104 100MHz CPU with a 10/100BaseT Fast Ethernet port, which provides up to 100Mbps network connectivity. A router connects all PC104 nodes, and a local area network (LAN) was established. Each node has a unique IP address in the LAN, and can send and receive data to and from each other via the TCP/IP protocol. The extensive data acquisition circuitry, including analog input channels, analog output channels, digital I/O channels, external triggers, and counters/timers, makes it convenient to connect the embedded controller directly to the sensors and actuators. The detailed specifications of the data acquisition circuit are listed in Table 2.

Table 2: Specifications of the Prometheus data acquisition circuit

Analog Inputs	
Number of inputs	16 single-ended or 8 differential (user selectable)
A/D resolution	16 bits (1/65536 of full scale)
Bipolar ranges	±10V, ±5V, ±2.5V, ±1.25V (software selectable)
Conversion rate	100,000 samples per second with interrupts
Analog Outputs	
Number of outputs	4 lines, Simultaneous update
D/A resolution	12 bits (1/4096 of full scale)
Output ranges	Fixed: ±10V, 0-10V (Programmable possible)

Five piezoceramic actuators were attached to the beam surface. The disturbance to the beam was generated through one of the actuators, and the other four served as control actuators. The placement of the actuators should also be considered just as the locations of sensors. The location of the actuator generating a disturbance to the beam was chosen to be 0.563m (the distance from the left end of the beam to the center of the actuator), and the other four were placed at the same locations as the sensors. The voltage from the D/A circuit in the microcontroller was amplified through a power amplifier, and the amplified control voltage drove the control actuators.

The system identification of the structure was performed before the design of the controller. Since we are only interested in the frequency range 0-250Hz, white noise with a frequency range 0-250Hz was generated to excite the structure. The sensor outputs were acquired at the sampling frequency 600Hz. By comparing the measured frequency response of the structure and theoretical FEA model, it was shown that resonant peaks

matched well. This means that the boundary conditions, mass and stiffness of the beam are well simulated. However, some elements in the FE model had to be adjusted to reflect the effect of the electric circuits, sensors and actuators.

After the model of the structure was obtained, the controller was designed using the LQR algorithm described above. The distributed control system could then be implemented. When the decentralized control system is running, clocks on all nodes (including the one that only generates the disturbance) will first be synchronized. The clock synchronization was accomplished using Reference Broadcast Synchronization as follows [12]: each node obtains IP addresses of its neighboring nodes, then waits; a packet is broadcast to all nodes in the network; when the packet reaches the physical port of a node, the microprocessor begins to work. Since the nondeterministic processing of TCP and IP layers are not involved in the synchronization procedure, the time taken for a packet to be transported is very small and the synchronization has very high precision of within 10  $\mu$ s of error.

After the clock synchronization, each microprocessor will generate system interrupts periodically. During the interval, which is 1/600 sec for all nodes, user interrupt routines will run. The four sensor nodes will perform the following steps during the interrupt interval: acquire data from the sensor through the A/D circuit; send the data to the node on its immediate right; receive data from the node on its immediate left; calculate the control voltage using the local data and the data from its left-hand neighbor; and send the control voltage to the actuator through the D/A circuit. The node on the leftmost end of the beam only sends but does not receive data, and the control voltage will be calculated based on its own data. Similarly, the node at the rightmost end of the beam only receives but does not send data. In our experimental setup, the voltage from the D/A circuit is filtered through a low-pass filter with a cutoff frequency of 600Hz in order to minimize the sensor noise at the accelerometer.

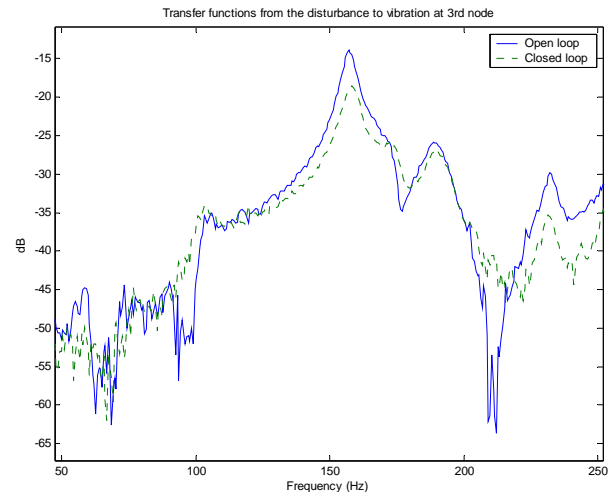


Figure 4: Transfer functions of open-loop system and closed-loop system

The performance of the distributed control system was evaluated by comparison of uncontrolled and controlled system

responses, which were in the frequency range of 0-250 Hz, the first six natural frequencies of the beam. The reduction of vibration responses of the system is shown in Fig. 4.

## CONCLUSION

In this paper decentralized vibration control of a simply supported beam has been implemented using networked embedded systems. It is shown that the reduction of system vibration is realized with a decentralized vibration control method. The approach used in this research can be extended to active noise control of other structures with networked embedded systems.

## ACKNOWLEDGEMENTS

This research was supported by the DARPA Information Exploitation Offices' Network Embedded System Technology (NEST) program and a National Science Foundation CAREER Award No. CMS-0134224.

## REFERENCES

- [1] Swigert, C. J. and Forward, R. L., 1981, "Electronic Damping of Orthogonal Bending Modes in a Cylindrical Mast - Theory," *Journal of Spacecraft and Rockets*, **18**, pp. 5-10.
- [2] Bailey, T. and Hubbard, J. E., Jr., 1985, "Distributed Piezoelectric Polymer Active Vibration Control of a Cantilever Beam," *Journal of Guidance, Control, and Dynamics*, **8**, pp. 605-611.
- [3] St-Amant, Y. and Cheng, L., 2000, "Simulations and experiments on active vibration control of a plate with integrated piezoceramics," *Thin-Walled Structures*, **38**, pp. 105-123.
- [4] Choi, S.-B., 1995, "Alleviation of chattering in flexible beam control via piezofilm actuator and sensor," *AIAA Journal*, **33**, pp. 564-567.

[5] Frampton, K. D., 2001, "Decentralized Control of Structural Acoustic Radiation," *Proceedings of Proceedings of IMECE 2001*, New York.

[6] Strassberger, M. and Waller, H., 2000, "Active noise reduction by structural control using piezo-electric actuators," *Mechatronics*, **10**, pp. 851-868.

[7] Hagood, N. W., Chung, W. H., and von Flotow, A., 1990, "Modelling of piezoelectric actuator dynamics for active structural control," *Proceedings of 31st AIAA/ASME/ASCE/AHS/ASC Structures, Structural Dynamics and Materials Conference*, Long Beach, CA, USA.

[8] Clark, R., Saunders, W., and Gibbs, G., 1998, *Adaptive Structures: Dynamics and Controls*, John Wiley & Sons, New York.

[9] Scholte, E. and D'Andrea, R., 2003, "Active Vibro-acoustic Control of a Flexible Beam Using Distributed Control," *Proceedings of 2003 American Control Conference, Jun 4-6 2003*, Denver, CO, United States.

[10] Balas, M. J., 1979, "Direct Velocity Feedback Control of Large Space Structures," *Journal of Guidance Control and Dynamics*, **2**, pp. 252-253.

[11] Levine, W. and Athans, M., 1970, "On the determination of the optimal constant output feedback gains for linear multivariable systems," *IEEE Transactions on Automatic Control*, **15**, pp. 44-48.

[12] Elson, J., Girod, L., and Estrin, D., 2002, "Fine-Grained Network Time Synchronization using Reference Broadcasts," *Proceedings of the Fifth Symposium on Operating Systems Design and Implementation*, Boston, MA.